

## Article

# Axial compression model for FRP confined concrete in elliptical cross sections

Zhenyu Wang<sup>1</sup>, Haytham F. Isleem<sup>2</sup>

<sup>1</sup>\*Professor, Harbin Institute of Technology, School of Civil Engineering, Harbin, 150090, China.

Corresponding Author E-mail: zhenyuwang@hit.edu.cn

<sup>2</sup>PhD Candidate, Harbin Institute of Technology, School of Civil Engineering, Harbin, 150090, China. E-mail: haythamisleem@hit.edu.cn

**Abstract:** Most of the existing studies conducted on FRP-confined concrete considered circular and square concrete columns, while limited studies were on columns with rectangular sections. The studies have confirmed that the circular cross-sections exhibited higher confinement effectiveness, whereas in the case of non-circular cross-sections the efficiency of FRP confinement decreases with an increase of the sectional aspect ratio and there is no significant increase, particularly for columns with the aspect ratio of 2.0. As recently suggested by the researchers, to significantly increase the effectiveness of FRP-confinement for these columns is by modifying a rectangular section to an elliptical or oval section. According to the literature, most of the existing confinement models for FRP-confined concrete under axial compression have been proposed for columns with circular and rectangular cross-sections. However, modeling the axial strength and strain of concrete confined with FRP in elliptical cross-sections under compression is most limited. Therefore, this paper provides new expressions based on limited experimental data available in the literature. For a sufficient amount of FRP-confinement, the threshold value was proposed to be 0.02. Finally, the accuracy of the proposed model was verified by comparing its predictions with the same test database, together with those from the existing models. .

**Keywords:** FRP confined; axial compression; RC columns; strength; ductility; modeling

---

## 1. Introduction

It is now well-recognized that confinement of existing concrete columns in bridges and buildings using fiber-reinforced polymers (FRPs) can significantly increase the strength and ductility of the columns. Over the last 25 years, a large number of experimental tests and analytical models were focused on the axial compressive behavior of FRP-confined concrete [e.g. 1-25]. The majority of the existing studies have focused on modeling the stress-strain behavior of FRP-confined concrete in circular cross-sections under axial compression, while only limited studies considered FRP-confined concrete in rectangular cross-sections [11-20].

Early research studies indicated that FRP confined square and rectangular sections with sharp corners provide only a little enhancement in their axial load capacities, while the confinement effectiveness increases directly with an increase in the corner radius (Wu and Zhou [21]). Meanwhile, the curvature of the rectangular section's corners could cause stress concentration (Al-Salloum [22]). Therefore, changing square section to circular section may minimize these stress concentration [23-29]. Only limited studies have been directed to changing a rectangular column section to an elliptical section [24, 25]. The first study of Yan [24] included an experimental program involved testing 30 FRP-confined concrete columns of circular, square and rectangular sections subjected to axial compressive loads. It was concluded that the FRP jackets are not able to effectively improve the compressive behavior of square and rectangular columns exhibiting a softening behavior. Recently it has been confirmed by Isleem et al. [16-18] for rectangular columns of larger-sized cross-sections that the confinement provided by the FRP wraps resulted in a significant improvement in axial strains but only a little improvement in axial strengths. In their study, the results of tests have shown that only the sufficiently confined

specimens with the aspect ratio of 1.5 reached higher strengths as compared with that of the unconfined concrete cylinder, while no strength enhancement was achieved for larger-sized specimens with the aspect ratio of 2.0. All experiments showed that the stress-strain curves of the confined columns exhibited a softening behavior in their response. The key solution to reduce the corner stress concentration that causes the softening behavior for such large-sized sections and thus to improve the strength and deformability of concrete columns with light and moderate confinement level is to modify the shape of square section to circular section and the rectangular cross-section to elliptical or oval cross-section using subsequent steel or composite jacketing [30-33]. Further, the shape modification method can also be employed when the corners of the rectangular section can no longer be rounded for fear of infringing on the minimum concrete cover for reinforcing steel bars (Parvin and Schroeder [34]).

The most economical method of shape modification of concrete columns is adding oval precast concrete segments to the perimeter of the rectangular column with subsequent FRP wrapping [34]. For this technique of modification of section's shape to be widely used for the strengthening of rectangular columns subject to axial compression, analytical expressions for predicting the axial strength and strain of FRP reinforced concrete columns with elliptical sections are needed. Because concretes in rectangular sections confined with FRP behave differently compared with the elliptical sections, if the available models of rectangular columns are directly applied to confined elliptical columns, the strength and strain capacities may not represent the realistic behavior of the columns, and unsafe design may be performed. Therefore, this paper aims to provide expressions for the accurate predictions of the axial strength and axial strain. In addition, based on the existing test database, the threshold for sufficiently confined concrete has been proposed to be equal to 0.02. This can be an important feature of the proposed model being able to predict well the threshold confinement condition that can dictate whether the stress-strain response ascends or descends. Finally, a good correlation was revealed between the predictions of the proposed model and the experimental test data.

## 2. Experimental Program

### 2.1. Overview of specimen details

In order to develop new strength and strain models, the the results of experimental tests performed by Teng and Lam [33] were used for the calibration of all expressions provided in this paper. Twenty unreinforced concrete specimens were prepared and tested under axial compression loading. The experimental tests included five groups of specimens (S1, S2, S3) divided according to their sectional aspect ratios  $a/b$  (1.0, 1.28, 1.7, 2.5) and prepared from the same batch of concrete as provided in Table 1. Each group included one specimen with a circular section and three elliptical specimens. The cross-sectional area and height of the elliptical specimens were almost equivalent to those of the circular sections. All of the specimens were 608 mm in height. The unconfined concrete strength was obtained from compressive tests on three cubes of 150 mm. Only the third and fourth groups as control specimens were considered without FRP confinement, while the other groups were confined with different numbers of layers of CFRP wraps. The variables considered in the tests were: (1) the sectional aspect ratio, (2) the batch of concrete, and (3) and the number of CFRP layers. As for the specimens' designation, S5/4L2, as an example, had a cross-sectional aspect ratio of 1.28 and was confined with two CFRP layers. The mechanical properties of the CFRP wraps are also provided in Table 1. Complete details of the tests are not provided in this paper; however, the researchers are directed to their reference.

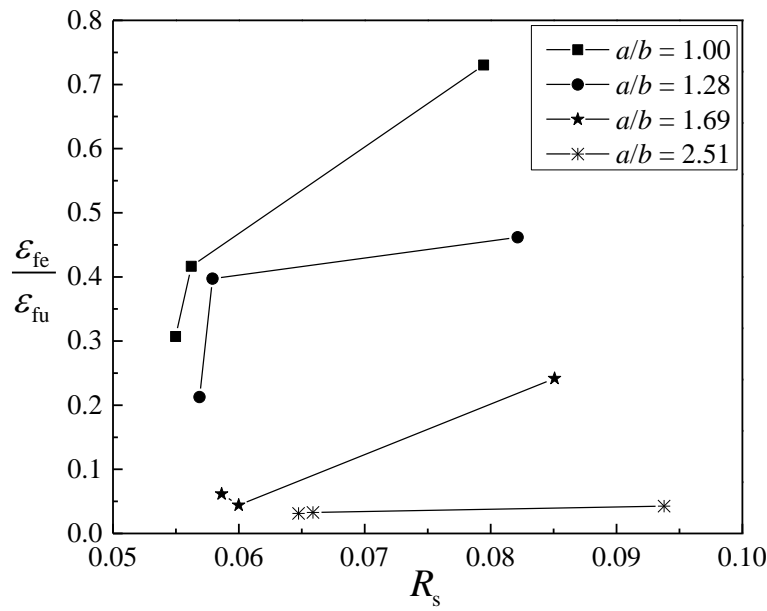


**Figure 1.** Effect of FRP confinement stiffness on hoop strain (Series 1 &5):  $\varepsilon_{fe}$  = average FRP hoop strain from gauges on minor and major section sides;  $\varepsilon_{fu}$  = FRP tensile strain obtained from flat test coupons

**Table 1.** Summary of FRP reinforcement, material and mechanical properties of test specimens.

| No.      | Specimen | Section details |             |       | Material Properties |                    |                |                |                           |  |
|----------|----------|-----------------|-------------|-------|---------------------|--------------------|----------------|----------------|---------------------------|--|
|          |          | $a$<br>(mm)     | $b$<br>(mm) | $a/b$ | $f'_c$<br>(MPa)     | $t_{wrap}$<br>(mm) | $f_f$<br>(MPa) | $E_f$<br>(GPa) | $\varepsilon_{fu}$<br>(%) |  |
| Series 1 |          |                 |             |       |                     |                    |                |                |                           |  |
| 1        | S1.0L1   | 152.2           | 152.2       | 1.00  | 48.8                | 0.165              | 3983           | 263            | 1.514                     |  |
| 2        | S5/4L1   | 168.2           | 131.6       | 1.28  | 48.8                | 0.165              | 3983           | 263            | 1.514                     |  |
| 3        | S5/3L1   | 194.8           | 115.6       | 1.69  | 48.8                | 0.165              | 3983           | 263            | 1.514                     |  |
| 4        | S5/2L1   | 237.6           | 94.8        | 2.51  | 48.8                | 0.165              | 3983           | 263            | 1.514                     |  |
| Series 2 |          |                 |             |       |                     |                    |                |                |                           |  |
| 5        | S1.0L1   | 151.6           | 151.6       | 1.00  | 47.1                | 0.110              | 3824           | 276            | 1.386                     |  |
| 6        | S5/4L1   | 168.4           | 131.6       | 1.28  | 47.1                | 0.165              | 3983           | 263            | 1.514                     |  |
| 7        | S5/3L1   | 194.9           | 114.8       | 1.70  | 47.1                | 0.165              | 3983           | 263            | 1.514                     |  |
| 8        | S5/2L1   | 236.5           | 95.0        | 2.49  | 47.1                | 0.165              | 3983           | 263            | 1.514                     |  |
| Series 3 |          |                 |             |       |                     |                    |                |                |                           |  |
| 9        | S1.0L0   | 151.9           | 151.9       | 1.00  | 43.5                | -                  | -              | -              | -                         |  |
| 10       | S5/4L0   | 168.5           | 131.6       | 1.28  | 43.5                | -                  | -              | -              | -                         |  |
| 11       | S5/3L0   | 194.8           | 115.9       | 1.68  | 43.5                | -                  | -              | -              | -                         |  |
| 12       | S5/2L0   | 237.8           | 94.6        | 2.51  | 43.5                | -                  | -              | -              | -                         |  |
| Series 4 |          |                 |             |       |                     |                    |                |                |                           |  |
| 13       | S1.0L0   | 152.0           | 152.0       | 1.00  | 44.6                | -                  | -              | -              | -                         |  |
| 14       | S5/4L0   | 168.7           | 131.4       | 1.28  | 44.6                | -                  | -              | -              | -                         |  |
| 15       | S5/3L0   | 194.8           | 115.0       | 1.69  | 44.6                | -                  | -              | -              | -                         |  |
| 16       | S5/2L0   | 236.8           | 94.6        | 2.50  | 44.6                | -                  | -              | -              | -                         |  |
| Series 5 |          |                 |             |       |                     |                    |                |                |                           |  |
| 17       | S1.0L2   | 152.3           | 152.3       | 1.00  | 45.8                | 0.220              | 3824           | 276            | 1.386                     |  |
| 18       | S5/4L2   | 168.2           | 131.9       | 1.28  | 45.8                | 0.220              | 3824           | 276            | 1.386                     |  |
| 19       | S5/3L2   | 194.8           | 115.0       | 1.69  | 45.8                | 0.220              | 3824           | 276            | 1.386                     |  |

|    |        |       |      |      |      |       |      |     |       |
|----|--------|-------|------|------|------|-------|------|-----|-------|
| 20 | S5/2L2 | 237.6 | 94.6 | 2.51 | 45.8 | 0.220 | 3824 | 276 | 1.386 |
|----|--------|-------|------|------|------|-------|------|-----|-------|

**Note:**  $a$  = width of a cross-section;  $b$  = depth of a cross-section;  $a/b$  = aspect ratio of a cross section;  $t_{\text{wrap}}$  = total thickness of FRP composite layers;  $f_f$  = maximum tensile strength of FRP composite;  $E_f$  = tensile elastic modulus of FRP composite;  $\varepsilon_{\text{fe}}$  = average FRP strain obtained using strain gauges installed on the FRP surface at the four vertices (minor and major section sides);  $\varepsilon_{\text{fu}}$  = FRP tensile strain obtained from flat test coupons;  $f'_c$  = compressive strength of unconfined concrete.

## 2.2. Overview of experimental test results

All the confined specimens failed by the rupture of the FRP wrap [33]. In most cases, the rupture happened at the upper or lower quarters of the specimens. The degree of damage for specimens with smaller aspect ratios was higher than that for specimens with larger aspect ratios. In addition, results have revealed that the confined strength is dependent on the amount of FRP confinement, which is resulted by the dependence of the FRP strain on the confinement stiffness ratio [35, 36]. Typical comparison of test results is presented in Figure 1. To take this parameter's effect into account, Equation 1 was first suggested by Teng et al. [37] for FRP-confined circular concrete columns and later modified by Pham and Hadi [38] for rectangular columns. In this paper, the following procedure to calculate the strength confinement ratio for the specimens in Table 1 was used.

$$(1) \quad R_s = \frac{\rho_f E_f}{f'_c / \varepsilon_{\text{co}}}$$

$$(2) \quad \rho_f = \frac{[3(a+b) - 2\sqrt{ab}]t_{\text{wrap}}}{ab}$$

$$(3) \quad \varepsilon_{\text{co}} = (-0.067f'_c^2 + 29.9f'_c + 1053) \times 10^{-6}$$

where  $\rho_f$  = volumetric ratio of FRP (Yan [24]);  $E_f$  = modulus of elasticity of FRP;  $\varepsilon_{\text{co}}$  = axial strain of unconfined concrete (Tasdemir et al. [39]);  $t_{\text{wrap}}$  = total thickness of FRP composite layers;  $f'_c$  = compressive strength of unconfined concrete.

The FRP hoop strains that occurred at the major axes were smaller than the strains measured at the minor axes. In this paper, the effective FRP strain (Equation 4) is used. Besides, it was reported that specimens with higher aspect ratios exhibited smaller FRP strains at peak load. Comparison of the test results of specimens with varying aspect ratios is shown in Figure 2, in which the FRP strain is found to decrease as the sectional aspect ratio increase, as it has been reported in several tests on confined concrete columns with rectangular sections [12, 16-18, 24]. Based on regression of the specimens results, Equation 5 with  $R^2$  value of approximately 91% is introduced.

$$(4) \quad \varepsilon_{\text{fe}} = k_\varepsilon \varepsilon_{\text{fu}}$$

where  $k_\varepsilon$  is a factor that considers the reduction in measured FRP hoop strain

$$(5) \quad k_\varepsilon = \frac{\varepsilon_{\text{fe}}}{\varepsilon_{\text{fu}}} = 83.21 \left( \frac{b}{a} \right)^{2.545} R_s^{1.856}$$

where the terms  $a$  and  $b$  are the width and depth of an elliptical cross-section, respectively.

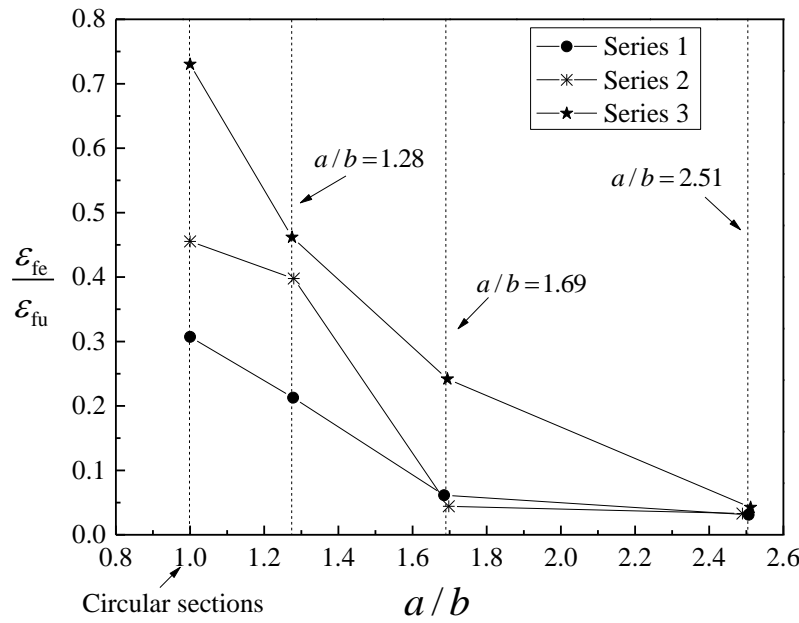


**Figure 2.** Effect of aspect ratio on FRP hoop strain:  $\varepsilon_{fe}$  = average FRP hoop strain from gauges on minor and major section sides;  $\varepsilon_{fu}$  = FRP tensile strain obtained from flat test coupons

**Table 2.** Published models of boundary value for sufficiently confined concrete.

| Published model    | Specimen type                     | Boundary value   |
|--------------------|-----------------------------------|------------------|
| Yan [24]           | Circular, rectangular, elliptical | $CR_1 \geq 0.20$ |
| Shao et al. [40]   | Circular                          | $CR_2 \geq 0.30$ |
| Pham and Hadi [38] | Circular, rectangular             | $CR_3 \geq 0.15$ |

**Table 3.** Comparison of published (Table 2) and proposed models for specimens in Table 1.

| Source/specimen    | S1.0L1     | S5/4L1     | S5/3L1     | S5/2L1     | S1.0L1     | S5/4L1     |
|--------------------|------------|------------|------------|------------|------------|------------|
| $f'_{cc}/f'_c$     | 1.240      | 1.096      | 0.852      | 0.770      | 1.166      | 1.157      |
| Yan [24]           | 0.047      | 0.034      | 0.020      | 0.002      | 0.049      | 0.035      |
| Evaluation         | unsuitable | unsuitable | satisfied  | satisfied  | unsuitable | unsuitable |
| Shao et al. [40]   | 0.125      | 0.126      | 0.119      | 0.105      | 0.087      | 0.131      |
| Evaluation         | unsuitable | unsuitable | satisfied  | satisfied  | unsuitable | unsuitable |
| Pham and Hadi [38] | 0.155      | 0.133      | 0.132      | 0.130      | 0.111      | 0.138      |
| Evaluation         | satisfied  | unsuitable | satisfied  | satisfied  | satisfied  | unsuitable |
| Proposed $MC_R$    | 0.067      | 0.020      | 0.011      | 0.005      | 0.072      | 0.021      |
| Evaluation         | satisfied  | satisfied  | satisfied  | satisfied  | satisfied  | satisfied  |
| Source/specimen    | S5/3L1     | S5/2L1     | S1.0L2     | S5/4L2     | S5/3L2     | S5/2L2     |
| $f'_{cc}/f'_c$     | 0.904      | 0.837      | 1.563      | 1.376      | 0.967      | 0.755      |
| Yan [24]           | 0.020      | 0.002      | 0.064      | 0.047      | 0.027      | 0.002      |
| Evaluation         | satisfied  | satisfied  | unsuitable | unsuitable | satisfied  | satisfied  |
| Shao et al. [40]   | 0.123      | 0.109      | 0.171      | 0.172      | 0.162      | 0.144      |
| Evaluation         | satisfied  | satisfied  | unsuitable | unsuitable | satisfied  | satisfied  |

|                    |            |            |           |           |            |            |
|--------------------|------------|------------|-----------|-----------|------------|------------|
| Pham and Hadi [38] | 0.137      | 0.135      | 0.204     | 0.171     | 0.175      | 0.172      |
| Evaluation         | unsuitable | unsuitable | satisfied | satisfied | unsuitable | unsuitable |
| Proposed $MC_R$    | 0.011      | 0.005      | 0.179     | 0.056     | 0.028      | 0.013      |
| Evaluation         | satisfied  | satisfied  | satisfied | satisfied | satisfied  | satisfied  |

If  $f'_{cc}/f'_c \geq 1.0$ , where the FRP confined specimen experienced enhancement in their axial strength and finally had an ascending stress-strain response, then the confinement pressure models in Table 2 are suitable. On contrary, for confined specimens with no strength enhancement  $f'_{cc}/f'_c < 1.0$ , the models are unsatisfied.

### 3. Effective confinement pressure ratio

As shown in Table 2, three analytical models for quantifying the effectiveness of FRP confinement for specimens with non-circular cross-sections were proposed in previous studies [24, 38, 40]. Based on their results, it was revealed that the strength increases by the increase of the ratio of the estimated confining pressure to the unconfined concrete strength (denoted as  $CR$  Table 3) being greater than a recommended value (For example 0.3 as reported by Shao et al. [40]). Details of the models can be found in their original papers.

Table 3 lists the effective confinement ratios from the proposed  $MC_R$  and existing models defined in this paper as  $CR$  ( $CR_{1,2,3}$  = model 1, 2, 3) for a total of 12 FRP-confined specimens selected from the paper of Teng and Lam [33]. As shown the models are not able to represent the actual results of their peak strengths. Therefore, based on the analysis of the database, the following expressions for estimating the FRP-confined peak strength and strain for elliptical columns are proposed in which the coefficient  $R^2$  value is approximately 93 and 94 %.

$$(6) \frac{f'_{cc}}{f'_c} = 0.62 + 1.88 \times (MC_R)^{0.39}$$

$$(7) \frac{\varepsilon_{cc}}{\varepsilon_{co}} = 1.0 + 26.59 \times (MC_R)^{0.89}$$

$$(8) MC_R = \frac{1}{2} k_e k_\varepsilon \frac{\rho_f E_f \varepsilon_{fu}}{f'_c}$$

where  $MC_R$  is a non-dimensionless coefficient used to account for the contributions of FRP confinement on the enhancement in ultimate strength experienced by the specimens;  $k_e$  is the FRP efficiency coefficient for elliptical sections (Figure 3). This was calculated using Equation 9, which was also used by Campione and Fossetti [41] but for estimating the confinement provided by the internal steel hoops.

$$(9) k_e = \frac{\pi ab - \left[ \frac{4}{3}b' \left( a - \frac{a'}{2} \right) + \frac{4}{3}a' \left( b - \frac{b'}{2} \right) + \frac{1}{3}(a'^2 + b'^2) \right]}{\pi ab}$$

where  $a'$  and  $b'$  are respectively the depth and width of a rectangular concrete block (Figure 5), referring to Campione and Fossetti [41] study.

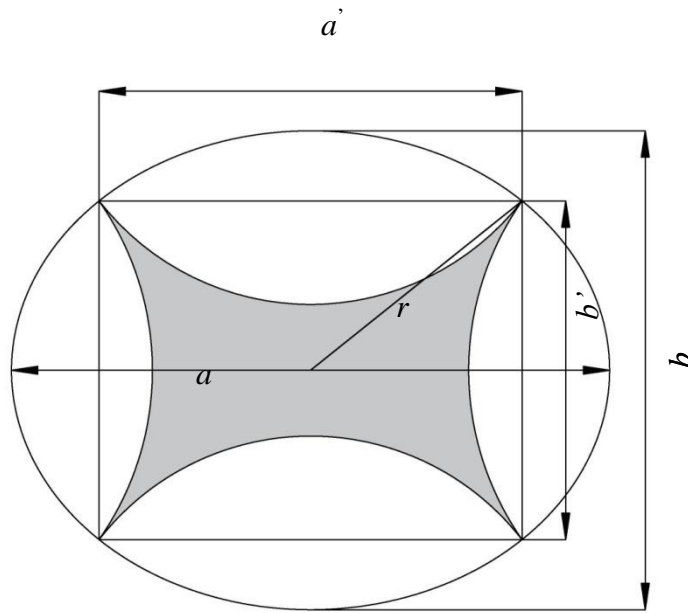


**Figure 3.** Effective confined area in elliptical-sectioned column

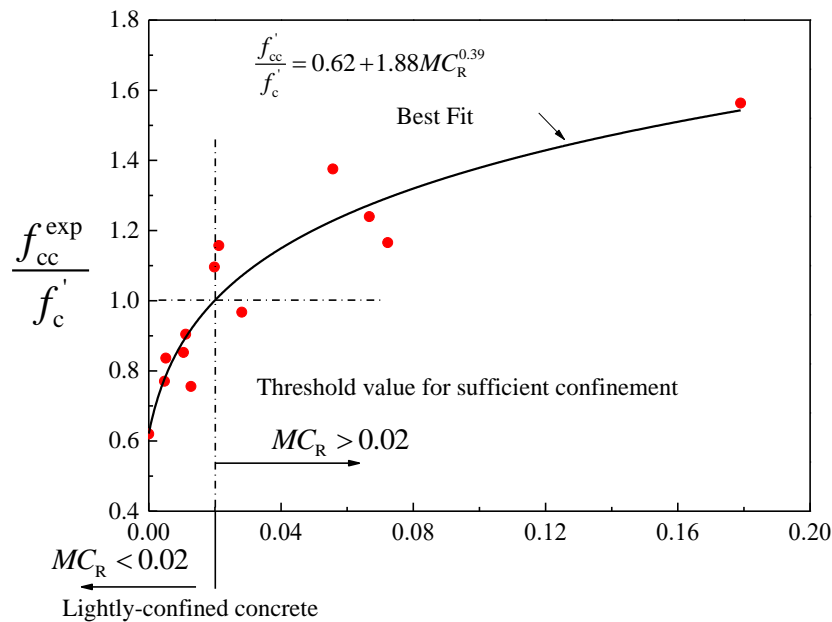


**Figure 4.** Relationship between effective confinement pressure ratio and ratio of the confined peak strength to the unconfined concrete strength

#### 4. Amount of FRP for sufficiently confined concrete

The studies on FRP-confined RC columns under compressive axial loads revealed that the internal reinforcement bars contribute to the increase of their strength and ductility [42-49]. In the studies, the confinement pressure was the sum of the confinement provided by the FRP wraps and that of the internal hoops. In earthquake-prone regions, a large number of RC columns, particularly of rectangular cross-sections, that were built based on the out-of-date codes may not have adequate lateral reinforcement to resist high seismic load levels (Isleem et al. [18]). As a result, they are subjected to major damages causing a total collapse of the building (Ilki et al. [50]).

Therefore, this discussion focuses on determining the following indicator that can ensure a sufficient confinement for the existing concrete columns. The relationship between  $MC_R$  and the ratio of the test peak strength to the strength of unconfined concrete was presented in Figure 4, in which the regressed line was only based on the results provided in Table 1 due to the unavailability of relative tests in the technical literature. Based on the regressed line, when  $f'_{cc}/f'_c = 1.0$ , the value of  $MC_R$  is equal to 0.02. When the  $MC_R$  is greater than the value of 0.02, then  $f'_{cc}/f'_c > 1.0$ , which means the  $f'_{cc}$  is greater than  $f'_c$ , and as a result, the confined specimen experienced enhancement in their strength and finally an ascending stress-strain response. Conversely, when the value of  $MC_R$  is less than 0.02, a second post-peak softening component occurs in the stress-strain response as reported in several tests conducted on columns in the literature (Isleem et al. [16-18]).

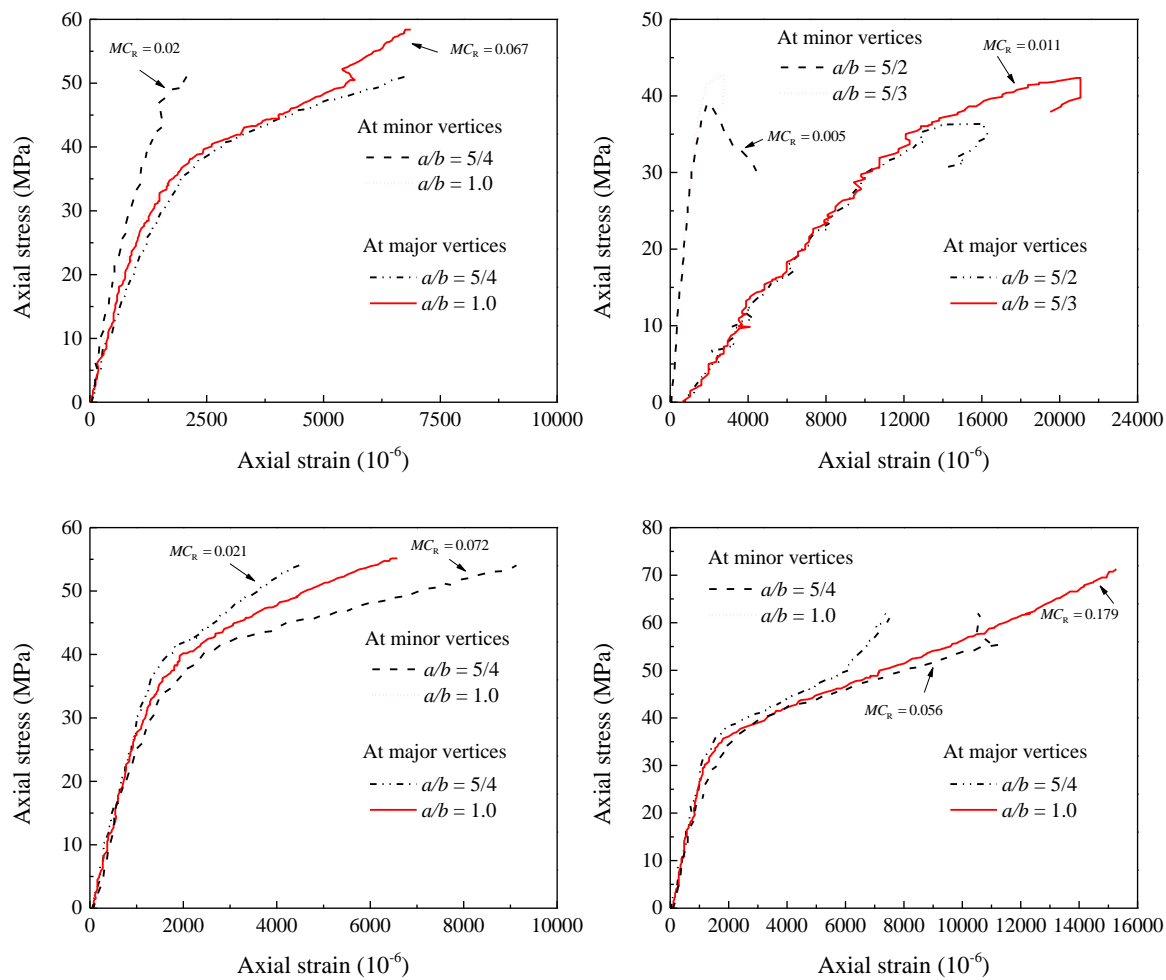


**Figure 5.** Accuracy of the proposed confinement pressure model  $MC_R$  against stress-strain test responses of specimens reported in Table 1

In the next section, the overall performance of the proposed and existing models of peak strength and strain of FRP-confined rectangular columns were evaluated against the results of columns with elliptical sections (Table 1). In the current discussions, the newly proposed confining pressure ratio is further checked through comparisons between the stress-strain test results of specimens in Table 1 and analytical values from the model. For more details of the selected tests, the readers are motivated to their original sources. These results were selected for the following reasons: (1) they had varying aspect ratios of cross-sections; (2) they had different strength of unconfined concrete; and (3) they had different confinement levels of FRP. In general, comparison of the test results with the predicted  $MC_R$

ratios provided in Figure 5 indicates that the confinement pressure model can distinguish between the different ascending and descending responses.

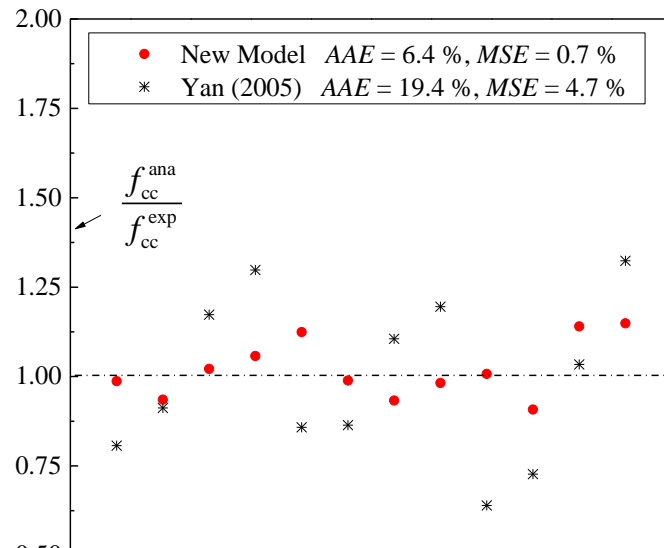
## 5. Accuracy of the proposed and existing strength and strain models

The performance of models that are capable of predicting the confined strength and strain enhancements achieved for elliptical columns due to the FRP confinement are assessed against the results summarized in Table 1. The two indicators namely (1) the average absolute error (*AAE*) (Equation 10) and (2) the mean square error (*MSE*) (Equation 11) are considered to establish the model accuracy. It can be generally observed from the comparisons in Figure 6 that the analytical values from the proposed Equations 6 and 7 agree well with the test results compared with the model of Yan [24]. It should be noted that there are no other comparisons in the figure with other experimental results and models due to the very limited research on the axial compressive behavior of FRP confined elliptical columns.

$$(10) AAE = \frac{\sum_{i=1}^n \left| \frac{\text{mod}_i - \text{exp}_i}{\text{exp}_i} \right|}{N}$$

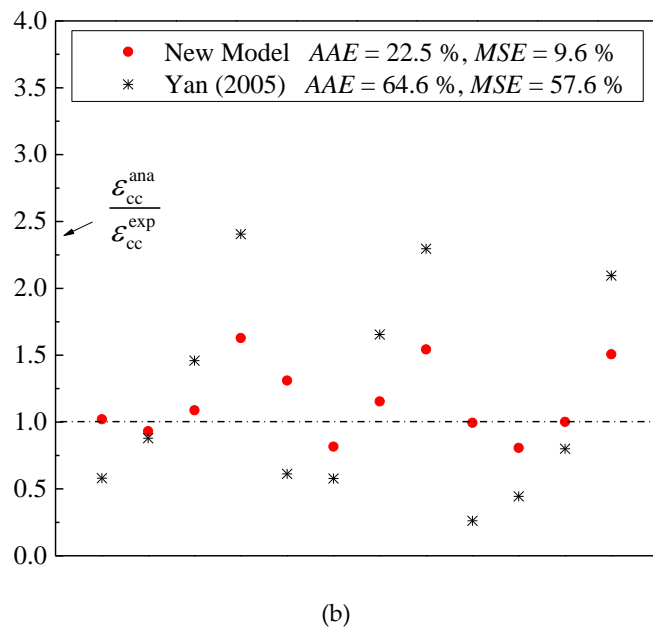
$$(11) MSE = \frac{\sum_{i=1}^n \left( \frac{\text{mod}_i - \text{exp}_i}{\text{exp}_i} \right)^2}{N}$$

Where  $(\text{mod}_i - \text{exp}_i)$  = the difference between the predicted value by the proposed model and that measured for the tested specimen  $i$ ;  $N$  is the total number of tested specimens.



(a)

**Figure 6.** Evaluation of proposed model and that of Yan (2005) against the results of peak axial strength (a) and peak axial strain (b)



(b)

**Figure 6. Cont.**

## 6. Conclusions

The existing tests and analytical models conducted on the axial compressive behavior of FRP-confined concrete have been largely concerned with columns of circular sections, where the concrete exhibited higher confinement due to uniform distribution of lateral stresses. On the contrary, the stress distribution in the case of a rectangular column varies over its cross section. Generally, the efficiency of FRP wraps decreases as the cross-sectional aspect ratio increases. Significant enhancements in ultimate strengths over the strength of unconfined concrete were achieved for columns with an aspect ratio of less than 2.0. In particular, columns with the aspect ratio equals to 2.0 were to experience a reduction in their ultimate strengths. The effectiveness of FRP confinement in terms of enhancement in ultimate strength can be significantly improved by the shape modification method. On the basis of the evaluation of existing models, it was revealed that the models available for rectangular FRP-confined specimens do not predict well the results of FRP-confined concrete in elliptical sections. Based on a regression analysis of the existing test results, a new model was presented to estimate the confined strength and strain of FRP-confined concrete columns having elliptical cross-sections. Based on the proposed model and the assembled test data, the threshold value of 0.02 for sufficiently confined elliptical concrete columns was proposed. Exceeding this value dictates the post-peak curve of the stress-strain response exhibits hardening behavior. The proposed model better predicted the test results compared with the predictions from the existing models for FRP-confined rectangular columns.

The model of this study is provided based on limited tests. Since the stress-strain behavior of FRP-confined columns is dependent on several parameters as discussed by many researchers, the model may not be applicable to parameters that are out of the range considered in the study. More research work for expanding its application should consider the effects of the internal hoop steel reinforcement on elliptical RC columns with larger section sizes as commonly used in practice.

## Acknowledgments

The second writer wishes to greatly acknowledge the financial support for the Ph.D. study obtained from the China Postdoctoral Science Foundation and the support of the National Natural Science Foundation of China.

### Notation

$a$  &  $b$  = width and depth of an elliptical section  
 $a/b$  = aspect ratio of an elliptical cross-section  
 $t_{\text{wrap}}$  = thickness of FRP composite layers  
 $E_f$  = tensile elastic modulus of FRP composite  
 $f_f$  = FRP maximum tensile strength  
 $\varepsilon_{fu}$  = FRP ultimate strain at rupture  
 $f'_c$  = strength of unconfined concrete  
 $\rho_f$  = volumetric ratio of FRP wraps  
 $\varepsilon_{co}$  = axial strain of unconfined concrete  
 $\varepsilon_{fe}$  = effective FRP hoop strain  
 $k_\varepsilon$  = efficiency factor for determining the FRP rupture strain  
 $k_e$  = coefficient for effectiveness of FRP confinement  
 $CR$  or  $MC_R$  = FRP confinement pressure ratio  
 $f'_{cc}$  = FRP-confined peak strength  
 $\varepsilon_{cc}$  = confined strain of confined concrete  
 $AAE$  = average absolute error  
 $MSE$  = mean square error  
 $N$  = total number of tested specimens  
 $ana$  = analytical value given by the model  
 $exp$  = experimental value obtained from tests

### References

1. Moran, D.A.; Pantelides, C.P. Stress-strain model for fiber-reinforced polymer-confined concrete. *J. Compos. Constr.* **2002**, *6*, 233-240.
2. Ilki, A.; Kumbasar, N. Behavior of damaged and undamaged concrete strengthened by carbon fiber composite sheets. *Struct. Eng. Mech.* **2002**, *13*, 75-90.
3. Albanesi, T.; Nuti, C.; vanzi, I. Closed form constitutive relationship for concrete filled FRP tubes under compression. *Const. Build. Mater.* **2007**, *21*, 409-427.
4. Vintzileou, E.; Panagiotidou, E. An empirical model for predicting the mechanical properties of FRP-confined concrete. *Const. Build. Mater.* **2008**, *22*, 841-854.
5. Lignola, G.P.; Prota, A.; Manfredi, G.; Cosenza, E. Unified theory for confinement of RC solid and hollow circular columns. *Compos. Part B-Eng.* **2008**, *39*, 1151-1160.
6. Micelli, F.; Modarelli, R. Experimental and analytical study on properties affecting the behaviour of FRP-confined concrete. *Compos. Part B-Eng.* **2013**, *45*, 1420-1431.
7. Lim, J.C.; Ozbakkaloglu, T. Unified stress-strain model for FRP and actively confined normal-strength and high-strength concrete. *J. Compos. Constr.* **2015**, *19*, 1-14.
8. Cascardi, A.; Micelli, F.; Aiello, M.A. Unified model for hollow columns externally confined by FRP. *Eng. Struct.* **2016**, *111*, 119-130, DOI: 10.1016/j.engstruct.2015.12.032.

9. Cascardi, A.; Micelli, F.; Aiello, M.A. An artificial networks model for the prediction of compressive strength of FRP-confined concrete circular columns. *Eng. Struct.* **2017**, *140*, 199-208.
10. Sadeghian, P.; Fillmore, B. Strain distribution of basalt FRP-wrapped concrete cylinders. *Case Studies in Construction Materials*. **2018**, <https://doi.org/10.1016/j.cscm.2018.e00171>.
11. Lam, L.; Teng, J.G. Design-oriented stress-strain model for FRP-confined concrete in rectangular columns. *J. Reinf. Plast. Compos.* **2003**, *22*, 1149-1186, <https://doi.org/10.1177/0731684403035429>.
12. Anselm, E. *Stress-strain behavior of rectangular columns confined with FRP sheets*. M.S thesis, University of Alabama, Huntsville, Al, 2005.
13. Pham, T.M.; Hadi, M.N.S. Stress prediction model for FRP confined rectangular concrete columns with rounded corners. *J. Compos. Constr.* **2014**, DOI: 10.1061/(ASCE)CC.1943-5614.0000407.
14. Triantafyllou, G.G.; Roisakis, T.C.; Karabinis, A.I. Axially loaded reinforced concrete columns with a square section partially confined by light GFRP straps. *J. Compos. Constr.* **2014**, *19*, DOI: 10.1061/(ASCE)CC.1943-5614.0000496.
15. Triantafillou, T.C.; Choutopoulou, E.; Fotaki, E.; Skorda, M.; Stathopoulou, M.; Karlos, K. FRP confinement of wall-like reinforced concrete columns. *Mater. Struct.* **2015**, DOI 10.1617/s11527-015-0526-5.
16. Isleem, H.F.; Wang, D.Y.; Wang, Z.Y. A new numerical model for polymer-confined rectangular concrete columns. *Proceedings of the Institution of Civil Engineers ICE: Struct. Build.* **2018a**, <https://doi.org/10.1680/jstbu.17.00103>.
17. Isleem, H.F.; Wang, D.Y.; Wang, Z.Y. Modeling the axial compressive stress-strain behavior of CFRP-confined rectangular RC columns under monotonic and cyclic loading. *Compos. Struct.* **2018b**, *185*, 229-240, <https://doi.org/10.1016/j.compstruct.2017.11.023>.
18. Isleem, H.F.; Wang, Z.Y.; Wang, D.Y.; Smith, S.T. Monotonic and cyclic axial compressive behavior of CFRP-confined rectangular RC columns. *J. Compos. Constr.* **2018c**, *22*, 292-300, DOI: 10.1061/(ASCE)CC.1943-5614.0000860.
19. Isleem, H.F.; Wang, D.Y.; Wang, Z.Y. Axial stress-strain model for square concrete columns internally confined with GFRP hoops. *Mag. Concr. Res.* **2018d**, *70*, 1064–1079.
20. Isleem, H.F.; Wang, Z.Y. A new strength prediction model for rectangular RC columns strengthened with CFRP wraps and anchors. *Proceedings of the Institution of Civil Engineers: Struct. Build.* **2018e**, under review.
21. Wu, Y.F.; Zhou, Y.W. Unified strength model based on Hoek-Brown failure criterion for circular and square concrete columns confined by FRP. *J. Compos. Constr.* **2010**, *14*, 175-184, DOI: 10.1061/(ASCE)CC.1943-5614.0000062.
22. Al-Salloum, Y.A. Influence of edge sharpness on the strength of square concrete columns confined with FRP composite laminates. *Compos. Part B-Eng.* **2007**, *38*, 640-650.
23. Tsai, K.C.; Lin, M.L. Seismic jacketing of RC columns for enhanced axial load carrying performance. *Journal of the Chinese Institute of Engineers.* **2002**, *25*, 389-402, <https://doi.org/10.1080/02533839.2002.9670714>.
24. Yan, Z.H. *Shape modification of rectangular columns confined with FRP composites*. Ph.D. Thesis, University of Utah, Salt Lake County, UT, 2005.

25. Pantelides, C.P.; Yan, Z. Confinement model of concrete with externally bonded FRP jackets or posttensioned FRP shells. *J. Struct. Eng.* **2007**, *133*, 1288-1296, DOI: 10.1061/(ASCE)0733-9445(2007)133:9(1288).
26. Yan, Z.; Pantelides, C.P. Concrete column shape modification with FRP shells and expansive cement concrete. *Const. Build. Mater.* **2011**, *25*, 396-405, DOI: 10.1016/j.conbuildmat.2010.06.013.
27. Xu, L. *Shape modification of square reinforced concrete columns confined with fiber-reinforced polymer and steel straps*. M.S thesis, University of Wollongong, Australia, 2012.
28. Zeng, J.J.; Guo, Y.C.; Gao, W.Y.; Li, J.Z.; Xie, J.H. Behavior of partially and fully FRP-confined circularized square columns under axial compression. *Const. Build. Mater.* **2017**, *152*, 319-332, <https://doi.org/10.1016/j.conbuildmat.2017.06.152>.
29. Jameel, M.T.; Sheikh, M.N.; Hadi, M.N.S. Behaviour of circularized and FRP wrapped hollow concrete specimens under axial compressive load. *Compos. Struct.* **2017**, *171*, 538-548, <https://doi.org/10.1016/j.compstruct.2017.03.056>.
30. Priestley, M.J.N.; Seible, F.; Xiao, Y.; Verma, R. Steel jacket retrofitting of reinforced concrete bridge columns for enhanced shear strength-Part 1: Theoretical considerations and test design. *ACI Struct. J.* **1994**, *91*, 394-405.
31. Priestley, M.J.N.; Seible, F. Design of seismic retrofit measures for concrete and masonry structures. *Const. Build. Mater.* **1995**, *9*, 365-377, [https://doi.org/10.1016/0950-0618\(95\)00049-6](https://doi.org/10.1016/0950-0618(95)00049-6).
32. Mandal, S.K.; Mansur, M.A. Strength and ductility of concrete confined by external wrap. *ACI Special Publication (SP200-42)*. **2001**, *200*, 677-692.
33. Teng, J.G.; Lam, L. Compressive behavior of carbon fiber reinforced polymer-confined concrete in elliptical columns. *J. Struct. Eng.* **2002**, *128*, 1535-1543, [https://doi.org/10.1061/\(ASCE\)0733-9445\(2002\)128:12\(1535\)](https://doi.org/10.1061/(ASCE)0733-9445(2002)128:12(1535)).
34. Parvin, A.; Schroeder, J.M. Investigation of eccentrically loaded CFRP-confined elliptical concrete columns. *J. Compos. Constr.* **2008**, *12*, 93-101, [https://doi.org/10.1061/\(ASCE\)1090-0268\(2008\)12:1\(93\)](https://doi.org/10.1061/(ASCE)1090-0268(2008)12:1(93)).
35. Rochette, P.; Labossière, P. Axial testing of rectangular column models confined with composites. *J. Compos. Constr.* **2000**, *4*, 129-136.
36. Wang, Z.Y.; Wang, D.Y.; Smith, S.T.; Lu, D.G. CFRP-confined square RC columns. I: Experimental investigation. *J. Compos. Constr.* **2012**, *16*, 150-160, DOI: 10.1061/(ASCE)CC.1943-5614.0000245.
37. Teng, J.G.; Jiang, T.; Lam, L.; Luo, Y.Z. Refinement of a design-oriented stress-strain model for FRP-confined concrete. *J. Compos. Constr.* **2009**, *13*, 269-278, DOI: 10.1061/(ASCE)CC.1943-5614.0000012.
38. Pham, T.M.; Hadi, M.N.S. Stress prediction model for FRP confined rectangular concrete columns with rounded corners. *J. Compos. Constr.* **2014**, DOI: 10.1061/(ASCE)CC.1943-5614.0000407.
39. Tasdemir, M.A.; Tasdemir, C.; Akyüz, S.; Barr, B.I.G. Evaluation of strains at peak stresses in concrete: A three-phase composite model approach. *Cem. Concr. Compos.* **2009**, *20*, 301-318, DOI: 10.1016/S0958-9465(98)00012-2.
40. Shao, Y.; Zhu, Z.; Mirmiran, A. Cyclic modeling of FRP-confined concrete with improved ductility. *Cem. Concr. Compos.* **2006**, *28*, 959-968, <https://doi.org/10.1016/j.cemconcomp.2006.07.009>.

41. Campione, G.; Fossetti, M. Compressive behaviour of concrete elliptical columns confined by single hoops. *Eng. Struct.* **2007**, *29*, 408-417, <https://doi.org/10.1016/j.engstruct.2006.05.006>.
42. Karantzikis, M.; Papanicolaou, C.G.; Antonopoulos, C.P.; Triantafillou, T.C. Experimental Investigation of Nonconventional Confinement for Concrete Using FRP. *J. Compos. Constr.* **2005**, *9*, 480-487.
43. Bournas, D.A.; Triantafillou, T.C. Bar Buckling in RC Columns Confined with Composite Materials. *J. Compos. Constr.* **2011**, *15*, 393-403.
44. Rousakis, T.C.; Karabinis, A.I. Adequately FRP confined reinforced concrete columns under axial compressive monotonic or cyclic loading. *Mater. Struct.* **2012**, *45*, 957-975.
45. Rousakis, T.C.; Tourtoutras, I.S. Modeling of passive and active external confinement of RC columns with elastic material. *J. Appl. Math. Mech.* **2015**, DOI 10.1002/zamm.201500014.
46. Bai, Y.L.; Dai, J.G.; Teng, J.G. Buckling of steel reinforcing bars in FRP-confined RC columns: An experimental study. *Const. Build. Mater.* **2017**, *140*, 403-415.
47. Zeng, J.J.; Lin, G.; Teng, J.G.; Li, L.J. Behavior of large-scale FRP-confined rectangular RC columns under axial compression. *Eng. Struct.* **2018**, *174*, 629-645.
48. Rousakis, T.C. Inherent seismic resilience of RC columns externally confined with nonbonded composite ropes. *Compos. Part B-Eng.* **2018**, *135*, 142-148.
49. Wan, B.; Jiang, C.; Wu, Y.F. Effect of defects in externally bonded FRP reinforced concrete. *Const. Build. Mater.* **2018**, *172*, 63-76.
50. Ilki, A.; Peker, O.; Karamuk, E.; Demir, C.; Kumbasar, N. FRP retrofit of low and medium strength circular and rectangular reinforced concrete columns. *J. Mater. Civ. Eng.* **2008**, *20*, 169-188, DOI: 10.1061/(ASCE)0899-1561(2008)20:2(169).